

Operation and performance of the Belle II Aerogel RICH detector

Kenta Uno^a

^a*Niigata University Niigata Japan*

Abstract

The Belle II experiment at the SuperKEKB asymmetric-energy e^+e^- collider is a B factory experiment to search for new phenomena beyond the Standard Model. One of the most important point in the experiment is a particle identification, especially the separation between kaons and pions. Thus, a proximity focusing Aerogel Ring Imaging Cherenkov (ARICH) counter is implemented in the forward endcap region to distinguish kaons and pions with momenta up to 4 GeV/c. The ARICH counter consists of a silica aerogel radiator and Hybrid Avalanche Photo Detector (HAPD). When a charged particle traverses the radiator, Cherenkov photons are emitted in the radiator and the emitted photons are detected by the HAPDs.

The Belle II experiment started the physics run in 2019 and accumulated 424 fb⁻¹ of collision data. The ARICH counter has been stably and the performance is consistent with our expectations. We report the detail of the operation of HAPDs and readout electronics. We also report the performance of ARICH counter using the data.

Keywords: ARICH counter, particle identification, photon detector

1. Introduction

The Belle II experiment at the SuperKEKB asymmetric-energy e^+e^- collider is a B factory experiment to search for new phenomena beyond the Standard Model. It aims to accumulate 50 times more data than its predecessor, Belle experiment and study rare decays with high precision such as $B \rightarrow \rho(\rightarrow \pi\pi)\gamma$ and $B \rightarrow K^*(\rightarrow K\pi)\gamma$. In order to search for these processes at Belle II, particle identification, especially the separation of charged kaons and pions is very important. In the Belle II detector, a proximity focusing Aerogel Ring Imaging Cherenkov (ARICH) counter as shown in Figure 1 is implemented to separate kaons from pions with momenta up to 4 GeV/c [1].

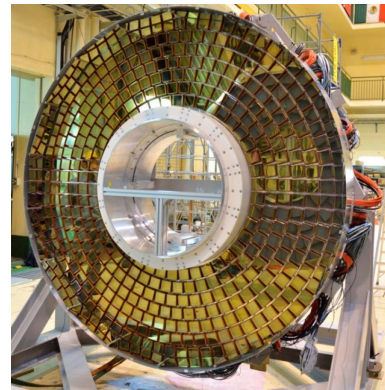


Figure 1: Photodetector plane of ARICH.

2. The ARICH counter

The ARICH counter consists of a silica aerogel radiator and Hybrid Avalanche Photo Detector (HAPD) as the photon detector. Figure 2 shows the principle of particle identification of the ARICH counter. When a charged particle traverses the radiator, Cherenkov photons are emitted in the radiator. Then, the emitted photons are detected by the photon detector. The emission angle of the Cherenkov photons is defined by $\cos\theta_C = \sqrt{(mc/p)^2 + 1}/n$, where θ_C is an emission angle of Cherenkov photon, m is the mass of the charged particle, p is the momentum of the charged particle and n is the refractive index of the aerogel radiator. Thus, it is possible to distinguish charged kaons from pions by using this angle.

The aerogel tile is 17×17 cm² size and 2 cm thickness. The ARICH counter is composed of 248 aerogel tiles and covers about 3.5 m² radiator plane. In order to improve the angle resolution, two aerogel layers with different refractive indices, $n_1 = 1.045$ and $n_2 = 1.05$, are introduced as shown in Figure 3.

The HAPD developed by Hamamatsu Photonics has a radiation tolerance up to the 1 MeV equivalent neutron dose of 10¹¹ cm⁻² per year and a good single photon detection with a magnetic field of 1.5 T. Figure 4 shows the HAPD module. A HAPD is composed of four Avalanche Photo Diode (APD) chips. Each APD chip has 6×6 pixels and a HAPD has 144 channels in total. The photon detection of the HAPD is based on the bombardment gain ($\mathcal{O}(1000)$) and the avalanche gain in the APD chip ($\mathcal{O}(10)$). A total of 420 HAPDs is used in the ARICH counter.

Email address: uno@hep.sc.niigata-u.ac.jp (Kenta Uno)

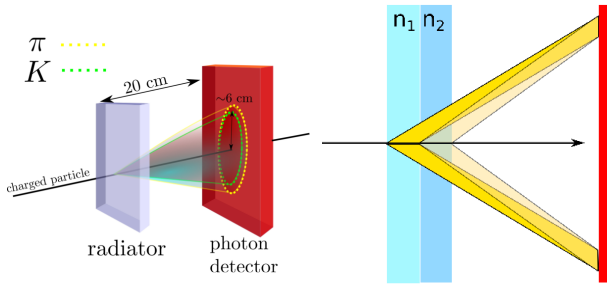


Figure 2: Principle of the particle identification of the ARICH counter.

Figure 3: Illustration of Cherenkov photon ring image using two layer scheme.

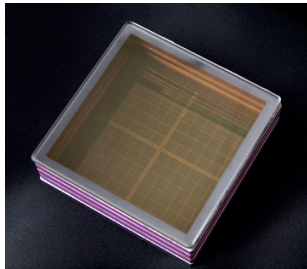


Figure 4: HAPD module

Signals from each HAPD are transmitted to the readout electronics in the ARICH counter. The readout electronics consist of Front-end board (FEB) and Merger board as shown in Figure 5. The FEB is attached to the HAPD and consists of Application Specific Integrated Circuit (ASIC) and the Xilinx Spartan-6 FPGA, where the hit information is digitized and transmitted to Merger boards. The Merger board consists of the Xilinx Vertex-5 FPGA and controls 5 or 6 FEBs. The main role of the Merger board is to combine the data of FEBs and transmit the data to the Belle II central data acquisition system.

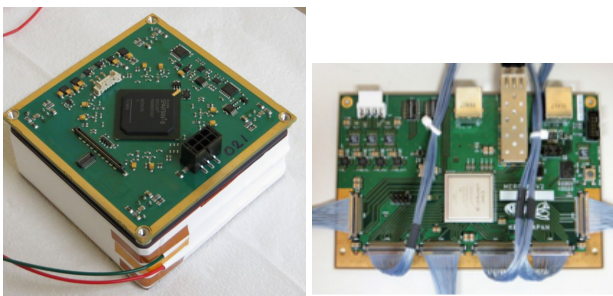


Figure 5: Readout electronics in the ARICH counter. Front-end board (left) and Merger board (right).

3. The operation of the ARICH counter

The Belle II experiment started the physics run with full detectors in 2019 and collected the data by June 2022 (Phase 3 run). We accumulated 424 fb^{-1} of collision data, which is almost equivalent to the BaBar dataset. Belle II has a world

record instantaneous luminosity of $\mathcal{L} = 4.7 \times 10^{34} \text{ cm}^{-2}\text{s}^{-1}$ in 2022. Several upgrades are currently performed to achieve higher luminosity. We plan to resume taking data in the next year.

The ARICH counter has been operated stably in Phase 3 run. Figure 6 shows the signal hit rate per channel during the physics run. A cluster of 5 dead HAPDs (1.2% of channels) is due to a connection failure of a low-voltage cable to the front-end electronics. It is fixed in this summer and thus, the HAPDs will be enabled in the next physics run. 3% of channels have problem inside APDs and we observe sudden increase of leakage current in the channels. 1.7% of channels have problem in the high-voltage cable. In total, 6% of channels have been disabled in the Phase 3 run. The number of the disabled channels is increasing every year, but it is getting stabilized. The impact on particle identification (PID) performance due to the disabled channels is negligible.

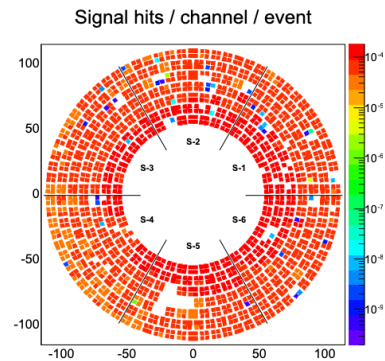


Figure 6: Signal hit rate per channel in the physics run.

In the Phase 3 run, we observe the deterioration of HAPDs due to silicon bulk damage by the neutron radiation, that is the increase of the leakage current. Figure 7 shows the leakage current of the APD between 2019 and 2022. The leakage current is increasing by around 30 nA per month. From this observation, the neutron fluence of $\sim 10^9 \text{ cm}^{-2}$ per month is expected. This is acceptable for the specification of the HAPD and we can continue the operation under high luminosity environment.

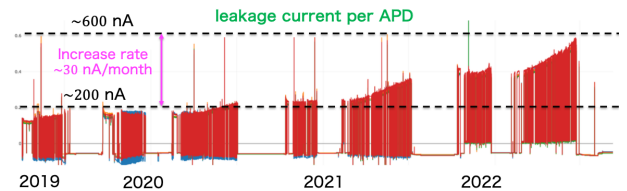


Figure 7: Leakage current of the APD between 2019 and 2022.

We also observe the single event upset (SEU) in the front-end electronics due to the neutron radiation. Frequent SEUs are expected in the Spartan-6 FPGA from the estimation based on the neutron irradiation test: ~ 8 SEUs per hour per FEB. The re-configuration of the firmware would be needed if SEUs happen.

Thus, the problem of SEUs is critical for a stable operation. In order to obtain a stable operation, we have implemented the scrubber of correcting radiation-induced errors in the merger firmware by majority voting across different module [3]. This process continuously runs and the partial reconfiguration of the firmware is performed if SEUs are detected. We have used this firmware from June 2020. Figure 8 shows the overview of the readout electronics and number of detected SEUs per 12 merger boards. The firmware detects and corrects SEUs day by day, but there is almost no failure caused by SEUs in the front-end electronics. As a result, we obtained the stable operation in the ARICH counter.

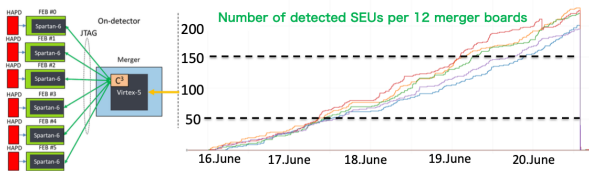


Figure 8: Overview of the readout electronics of ARICH counter (left) and number of detected SEUs per 12 merger boards (right).

It is also important to reduce errors and to make a quick recovery system to the errors. We utilize Elastalert, which is a third-party tool to implement alerting function, for better data taking efficiency. This tool always monitors all readout electronics based on log message and alert shifters if the errors happened. Thus, it is easily identify the source of the errors and provide how to fix them. We have implemented the system in 2021. In 2020, there were several errors during the physics run and the run stopped for about 6 hours in total. By introducing the quick recovery system, shifters can quickly fix the errors and the downtime can be significantly reduced that is, 1/6 or less than before. Assuming the luminosity of $\mathcal{L} = 4.0 \times 10^{34} \text{ cm}^{-2}\text{s}^{-1}$, the reduced downtime corresponds to $\sim 1.0 \text{ fb}^{-1}$ of data, that is large impact.

4. PID performance of the ARICH counter

A likelihood method is used for PID in the ARICH counter. It is based on the comparison between the observed hit pattern of Cherenkov photons and the expected probability density function (PDF) for the assumed charged particle hypothesis. We construct likelihood function for 6 type hypotheses ($h = e, \mu, \pi, K, p, d$). The likelihood function for a particle hypothesis (\mathcal{L}_h) is defined as

$$\ln \mathcal{L}_h = -N_h + \sum_i [n_{h,i} + \ln(1 - e^{-n_{h,i}})], \quad (1)$$

where $n_{h,i}$ is the expected number of hits on the i -th pixel and N_h is the expected total number of hits. The separation between kaons and pions is performed by applying a selection criteria on the likelihood ratio ($R_{K/\pi}$) defined as

$$R_{K/\pi} = \frac{\mathcal{L}_K}{\mathcal{L}_K + \mathcal{L}_\pi}, \quad (2)$$

$$R_{\pi/K} = \frac{\mathcal{L}_\pi}{\mathcal{L}_K + \mathcal{L}_\pi} = 1 - R_{K/\pi}. \quad (3)$$

We estimated PID performance with the samples $D^{*+} \rightarrow D^0(\rightarrow K^- \pi^+) \pi_{\text{slow}}^+$ using an integrated luminosity of 71.2 fb^{-1} and Monte Carlo (MC) simulation. The kaon and pion from D^0 decay can be purely reconstructed using the charge of slow pion π_{slow}^+ . Figure 9 shows the distribution of D^0 mass before and after applying $R_{K/\pi} > 0.5$ requirement for the pion and kaon track using the data. Applying the kaon identification, the kaon track is kept whereas the pion track is highly suppressed. Figure 10 shows receiver operating characteristic (ROC) between K efficiency and π mis-identification efficiency for the data and MC simulation. An agreement between data and MC simulation is observed within a few percent level and the study of the detector alignment and calibration is performed. We also calculated K efficiency and π mis-identification efficiency run by run to check the effect of PID performance on the beam-induced background as shown in Figure 11. The stable PID performance against beam-induced background is observed for the data and MC simulation.

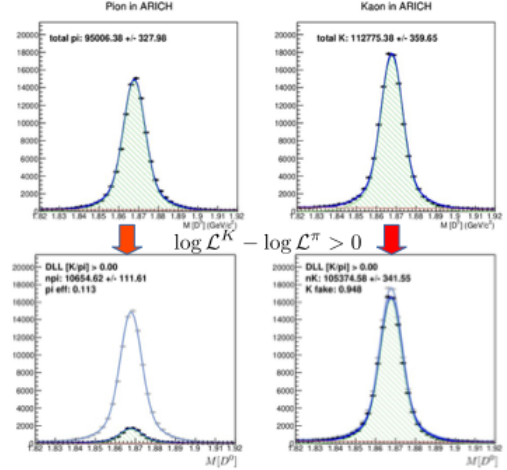


Figure 9: D^0 mass distribution in D^* sample before and after applying $R_{K/\pi} > 0.5$ requirement for the pion and kaon track using the data.

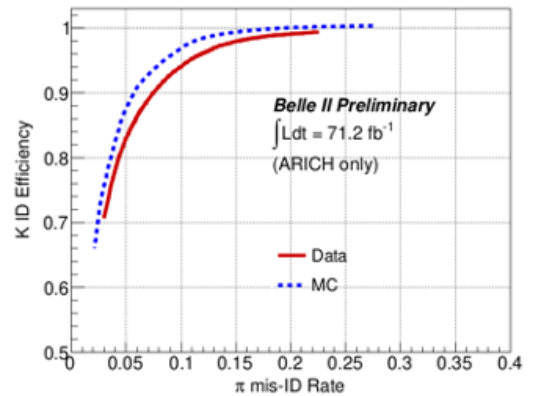


Figure 10: ROC curve for K efficiency and π mis-identification efficiency.

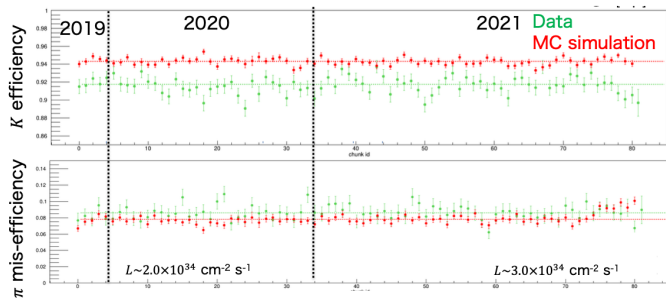


Figure 11: K efficiency and π mis-identification efficiency run by run.

5. Conclusion

The ARICH counter is a charged particle identification device in the forward endcap at the Belle II spectrometer. It uses a proximity focusing RICH counter and is designed to separate between kaon and pions with momenta up to $4 \text{ GeV}/c$ by Cherenkov ring imaging. The ARICH counter has been operated stably in Phase 3 run. The PID performance has been checked by using the data and the performance for the data is consistent with MC expectation. In order to improve the performance, we will study the detector alignment and calibration using more data.

References

- [1] T. Iijima, S. Korpar *et al.*, Nucl. Instrum. Meth. **A548**, (2005) 383
- [2] R. Giordano *et al.*, IEEE Trans. Nucl. Science, **68**, (2021).
- [3] R. Giordano *et al.*, arXiv:2010.16194.